We are IntechOpen, the world's leading publisher of Open Access books Built by scientists, for scientists

4,800
Open access books available

122,000
International authors and editors

135M
Downloads

Our authors are among the

154
Countries delivered to

TOP 1%
most cited scientists

12.2%
Contributors from top 500 universities

CLARIVATE ANALYTICS BOOK CITATION INDEX INDEXED

WEB OF SCIENCE™

Selection of our books indexed in the Book Citation Index in Web of Science™ Core Collection (BKCI)

Interested in publishing with us?
Contact book.department@intechopen.com

Numbers displayed above are based on latest data collected.
For more information visit www.intechopen.com

Chapter

Molecular Interactions in Ionic Liquids: The NMR Contribution towards Tailored Solvents

Mónica M. Lopes, Raquel V. Barrulas, Tiago G. Paiva, Ana S. D. Ferreira, Marcileia Zanatta and Marta C. Corvo

Abstract

Ionic liquids have been on the spotlight of chemical research field in the last decades. Their physical properties (low vapor pressure, thermal stability, and conductivity) and the possibility of fine tuning make them a versatile class of compounds for a wide range of applications, such as catalysis, energy, and material sciences. Ionic liquids can establish multiple intermolecular interactions with solutes such as electrostatic, van der Waals, or hydrogen bonds. The prospect of designing ionic liquid structures toward specific applications has attracted the attention to these alternative solvents. However, their rational design demands a molecular detailed view, and Nuclear Magnetic Resonance is a unique and privileged technique for this purpose, as it provides atomic resolution and at the same time enables the study of dynamic information. In this chapter, we provide an overview about the application of Nuclear Magnetic Resonance spectroscopy techniques as a methodology for the rational design of ionic liquids as solvents for small organic compounds, CO_2 capture, and polymers such as cellulose focusing mainly in the last 10 years.

Keywords: ionic liquids, nuclear magnetic resonance spectroscopy, molecular interactions, chemical shift deviations, nuclear Overhauser effect, solute/solvent

1. Introduction

Ionic liquids (ILs) can be defined as ionic species that melt under 100°C. These materials are usually made from organic cations such as imidazolium, ammonium, pyrrolidinium, or phosphonium, and organic or inorganic anions such as chloride, bromide, tetrafluoroborate, or bis(trifluoromethylsulfonyl)imide (**Figure 1**). Their physical properties, namely low vapor pressure, thermal stability, and conductivity grant them the status of alternatives to organic solvents in a wide range of applications, from catalysis and energy applications to material sciences. These properties are a direct consequence of the identity and interactions between the cations and the anions; however, the vast number of possible combinations hampers the tailoring of ILs as solvents for specific applications. In order to establish the desired structure-property relationships, a molecular understanding on structure and

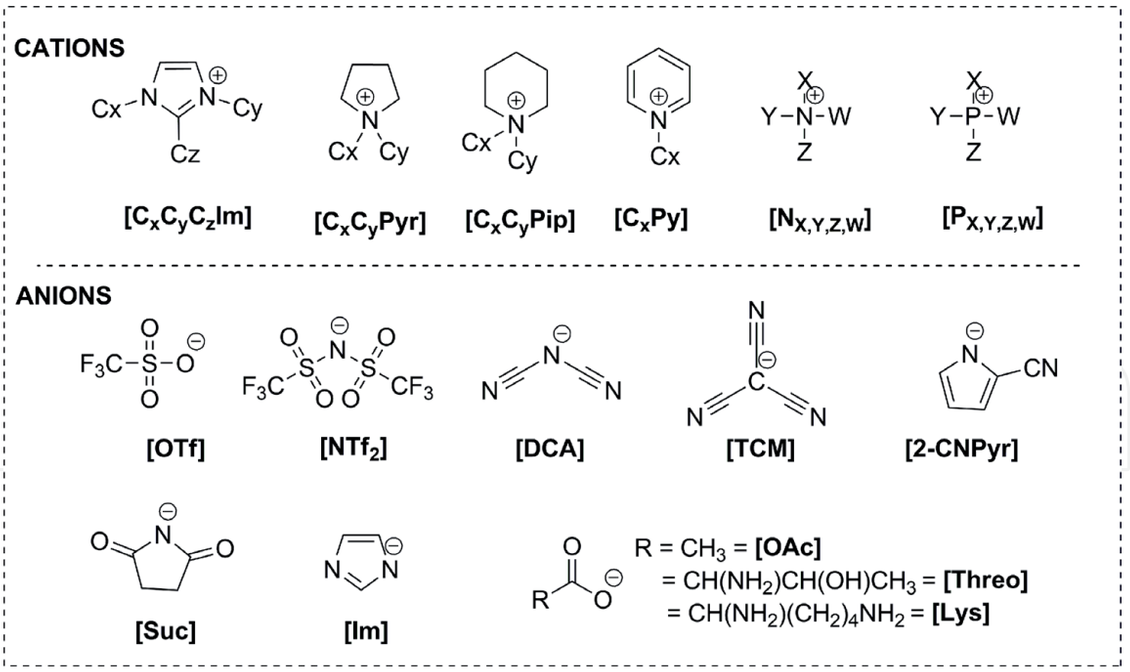

Figure 1.
Common cation and anion structure of ILs. The abbreviations used in this chapter are described in Section 7.

interactions is required. Nuclear Magnetic Resonance (NMR) techniques enable this study by allowing to probe both cations and anions through several nuclei (^{1}H, ^{13}C, ^{19}F, ^{35}Cl, ^{11}B, ^{15}N, and ^{31}P). In addition, the use of chemical shift deviations, relaxation, NOE, and diffusion experiments allows advanced studies about cation-anion-solute interactions and consequently facilitates the design and IL applications.

As solvents, ILs can establish several attractive interactions that range from weak, nonspecific, and isotropic forces such as van der Waals, solvophobic, and dispersion forces, to strong interactions as Coulombic forces and anisotropic forces such as hydrogen bonds (H-bonds), halogen bonds, dipole-dipole, magnetic dipole, and electron pair donor/acceptor interactions. The diversity and strength of intermolecular forces in ILs are responsible for the local arrangements in bulk and interface [1].

NMR enables the study of structure and dynamics in ILs providing information that allows the rationalization of the solvation behavior [2, 3]. Thus, by obtaining the profile of IL molecular interactions, it is possible to select and optimize the cation and anion identity and their relation to solvated species. In particular, the use of multinuclear NMR experiments and homo and heteronuclear correlation protocols enables the *in-situ* evaluation of cation-cation, cation-anion, anion-anion, and also IL-solute relationships.

In neat imidazolium ILs (ImILs), H-bonds are formed between the cation and the anion. This attractive force in which hydrogen nuclei are bound to electronegative atoms such as nitrogen, oxygen, or fluorine is mainly felt by the aromatic protons of the imidazolium cation (H_2, H_4, and H_5) and establishes a regular network. When a H-bond is formed, the hydrogen's electron density is pulled by an electronegative atom, leading to a deshielding of this nucleus and consequent positive chemical shift deviation ($\Delta\delta$). If a H-bond is weakened or broken, the opposite occurs, leading to a negative $\Delta\delta$. The addition of a solute to the IL can establish additional H-bonds and also introduce perturbations to the regular network, either reinforcing the interaction between cation and anion (positive $\Delta\delta$) or weakening (negative $\Delta\delta$) (**Figure 2I**) [4, 5].

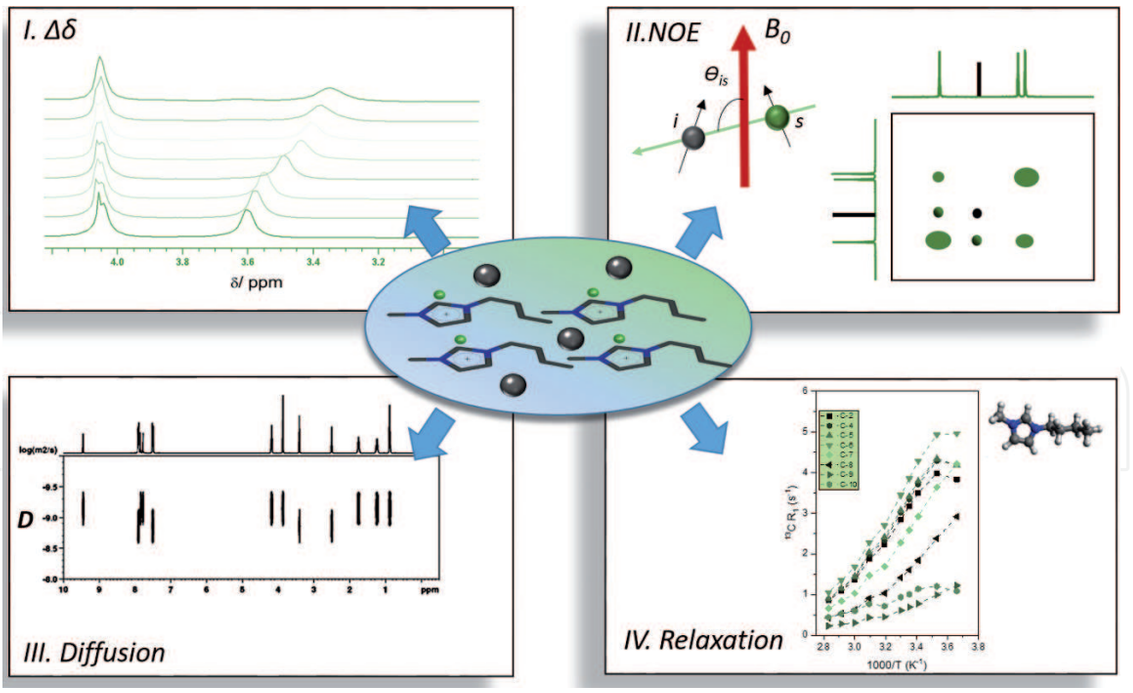

Figure 2.
NMR experimental techniques used to probe molecular interactions in ILs.

The nuclear Overhauser effect (NOE) is commonly used to study local structure in liquids and solutions. Considering the two nuclear spins, *I* and *S*, the magnetization transfer through coupling of their magnetic dipole moments produces a cross-relaxation and a consequent NOE (**Figure 2II**). Increasing the internuclear distance (r), the cross-relaxation rate decays with $1/r^6$. Thus, a NOE is only felt if r is less than 4–5 Å. Although this theory still holds for intramolecular distances, a new concept was introduced by Gabl et al. to analyze intermolecular NOE in ILs. According to these authors, the distance rule is strongly dependent on the frequencies of the interacting nuclei and can instead vary with $1/r$. Site-specific NOE should be interpreted cautiously as it can reflect the mean orientation of the ions over longer distances, rather than the local structure of distinct ion aggregates. Nevertheless, homonuclear (NOESY) and heteronuclear NOE (HOESY) studies have been widely used to analyze intermolecular interactions of solutes with ILs [6–8].

In ILs, the self-diffusion coefficients in solution can be measured through diffusion ordered spectroscopy (DOSY) providing a means to understand charge transport properties. In particular, using pulsed field gradient NMR (PFG-NMR), the spatial positions of the nuclei are encoded by magnetic field gradients, in which the signal intensity attenuation is correlated with the diffusion time (Δ) and the gradient-related parameters (g, δ) [9]. Multinuclear diffusion measurements can give access to anion and cation self-diffusion coefficients (**Figure 2III**); however, since ion-pair interactions take place on a timescale faster than the diffusion, the coefficients are a weighted average of charged and neutral species [10].

A deeper insight into atomic level interactions comes from NMR relaxation techniques (**Figure 2IV**). NMR spin-lattice (T_1) and spin-spin (T_2) relaxation measurements allow the study of reorientation dynamics in ILs and the analysis of inter- and intramolecular interactions [11–13].

Overall, probing intermolecular interactions in ILs through simple 1D NMR spectrum analysis (Δδ), or more complex relaxation phenomenon, NOE experiments, and diffusion provides an understanding of the interplay between ILs and solutes. The following sections highlight several examples where NMR techniques were used to tailor ILs.

2. Interactions between ionic liquids and small organic molecules

The optimization of liquid-liquid extraction processes for small organic molecules with organic solvents usually requires high investment and large energy consumption due to unfavorable capacity and selectivity [14]. Since this process is common in many industrial areas, more sustainable procedures are required in order to reduce organic solvent volatiles. Usually, an efficient separation of azeotropic systems containing the mixtures of aromatic/saturated hydrocarbons or alcohols/aliphatic hydrocarbons is difficult to obtain because of similar boiling points and several possible azeotropes. In this field, ILs have been cited as an alternative solvent, since they can provide an enhanced solvation capability while having negligible vapor pressure [14, 15]. The efficiency of ILs for absorption of aromatic compounds is determined by the size and structure of both cations and anions, as well as the molecular structure of the aromatic compounds. This section will focus on IL-aromatic molecule interactions consisting of two main groups: (i) unsubstituted and (ii) substituted aromatic molecules.

2.1 Unsubstituted aromatic molecules

Kumar and Banerjee reported that smaller IL cations enhanced the extraction capability for aromatic compounds [16]. Later, Potdar et al. studied binary mixtures of $[C_2C_1Im]^+$ with $[C_1SO_4]^-$, $[C_2SO_4]^-$, and $[C_1SO_3]^-$ as counterions to extract benzene from hexane, measuring the equilibrium compositions by ^1H NMR spectroscopy [14]. $[C_2C_1Im][C_2SO_4]$ achieved higher selectivity and capacity than IL binary mixtures. The combination of two ILs could result in lower free volume than a single IL, and benzene molecules would be unable to penetrate the core of the solvent.

Other studies in 2014 by Dias et al. reported interactions between benzene and $[C_2C_1Im][NTf_2]$, through several NMR experiments, namely, 1D ^1H and ^{13}C spectroscopy and 2D ^1H,^1H-NOESY spectroscopy [17]. In the mixture of benzene with $[C_2C_1Im][NTf_2]$, H_2 presented a lower chemical shift (more shielded) than neat IL, which indicated that the cation was positioned above and below the aromatic ring plane, and the anion was located in the same plane as benzene protons [17, 18]. Early works on the absorption of aromatic sulfur compounds by Su et al. studied the interaction between thiophene and $[C_4C_1Im][PF_6]$, $[C_4C_1Im][BF_4]$, and $[C_2C_1Im][BF_4]$, through 1D ^1H, ^{19}F, ^{11}B, and ^{31}P spectroscopy [19]. The ring current effect in neat thiophene was stronger than in neat $[C_4C_1Im][PF_6]$, because in the former, molecules were tightly packed, whereas in the IL, $[C_4C_1Im]^+$ cations were separated by $[PF_6]^-$ anions. The bulky $[PF_6]^-$ prevented $[C_4C_1Im]^+$ cations from coming close and reduced the aromatic current effect. In $[C_4C_1Im][PF_6]$/thiophene mixture, an upfield shift in $[C_4C_1Im]^+$ protons was explained as a result of the CH-π interaction between $[C_4C_1Im]^+$ and thiophene aromatic ring. The trend of $\Delta\delta$ indicated that $[C_4C_1Im]^+$ was in the shielding cone of thiophene ring current and the thiophene was located near the deshielding zone of $[C_4C_1Im]^+$ ring current. In addition, thiophene is not a good H-bond acceptor because the unpaired electrons of sulfur participate in the aromatic ring current and may carry a partial positive charge. The $[PF_6]^-$ anion was a potential hydrogen acceptor but introduced a downfield shift. The dilution of $[C_4C_1Im][PF_6]$ by a neutral molecule like thiophene was not expected to break apart the strong Coulombic interaction between $[C_4C_1Im]^+$ and $[PF_6]^-$ ions significantly by a simple insertion between them. The electric field effect risen from the physical interaction between fluoro-based anions and cations or thiophene was not a dominant factor in determining the IL absorption capacity for thiophene. The upfield shift effect was strongest for the ring protons in the imidazolium cation followed by the methyl and methylene protons next to the

nitrogen. The further away the protons were from the ring as in 1-butyl or 1-ethyl groups, the weaker the upfield shift effect became. Therefore, thiophene molecules must locate close to the ring of the IL's imidazolium cation. The CH-π interaction between the acidic hydrogen of cation and thiophene was not as important as the π (imidazolium ring)-π (thiophene ring) interaction. Apparently, the aromatic ring current effect (π-π interaction) is the dominant factor to determine the Δδ trend in these IL systems. The chain length of the imidazolium alkyl group and the size and character of anion affected the coordination number and geometric arrangement of thiophene molecules relative to IL's cations and anions. The stacking structure of the cation and anion was tightest for the neat $[C_2C_1Im][BF_4]$, followed by $[C_4C_1Im][BF_4]$ and $[C_4C_1Im][PF_6]$. Therefore, the negative charge of $[BF_4]^-$ anion in the $[C_2C_1IM][BF_4]$ was spread more around fluorine atoms and less around boron than those in the $[C_4C_1Im][BF_4]$ system. It also suggested that the $[BF_4]^-$ anion in the $[C_2C_1Im][BF_4]$ system is more basic and interacts more intimately with the imidazolium cation than in $[C_4C_1Im][BF_4]$. The NMR results suggested that the partial positive charge in thiophene sulfur should direct the anions outside the thiophene plane. Overall, the aromatic ring current interaction between the imidazolium cations and the thiophene was responsible for the absorption of aromatic sulfur compounds in ILs [19].

Revelli et al. studied the interaction of thiophene with $[C_1C_1Im][(C_1O)PHO_2]$ and $[C_4C_1Im][SCN]$, using ^1H and ^{31}P NMR spectroscopy [15]. The dilution of $[C_4C_1Im][SCN]$ by thiophene did not lead to a visible ^1H Δδ; therefore, thiophene did not break apart the strong Coulombic interactions between cation and anion. Indeed, phase equilibria of $[C_4C_1Im][SCN]$/thiophene system indicated that thiophene had low solubility in this IL. The acidic hydrogen atoms of the imidazolium cation formed weak H-bonds with the sulfur of thiocyanate anions. ^1H NMR chemical shifts of the ring protons in neat thiophene were more upfield than those in neat $[C_4C_1Im][SCN]$, indicating, as previously, that the aromatic ring current effect was stronger in neat thiophene than in neat $[C_4C_1Im][SCN]$. The bulky $[SCN]^-$ anion prevented the $[C_4C_1Im]^+$ cation from coming close, thus greatly reducing the aromatic current effect. Similar studies were made to unveil the interactions between thiophene and $[C_1C_1Im][(C_1O)PHO_2]$. The Δδ of thiophene and $[C_1C_1Im][(C_1O)PHO_2]$ followed the same trend as in $[C_4C_1Im][SCN]$. The chemical shifts of thiophene protons were more downfield when the thiophene is in a mixture of IL, although the IL proton chemical shifts were upfield. The ^{31}P chemical shifts were measured at several molar ratios of thiophene in $[C_1C_1Im][(C_1O)PHO_2]$, but no Δδ was observed; hence, the interactions between thiophene and anion are weak. The most prominent features in the vicinity of thiophene are an excess of cations in the polar regions above and below the ring and an excess of anions around the equator of thiophene. In the end, $[C_4C_1Im][SCN]$ is a promising IL to act as a solvent for desulfurization [15].

Kaintz et al. contributed to the measurements of solute diffusion in IL solutions through infinite dilution, since it eliminates solute-solute interactions. The authors studied the interactions between $[C_nC_1Pyr][NTf_2]$ (n = 3, 4, 6, 8, and 10) and $[P_{6,6,6,14}][NTf_2]$ and naphthalene, anthracene, pyrene, and biphenyl, through pulsed field gradient ^1H NMR. Within the selected set of aromatic solutes and pyrrolidinium ILs, no dependence was found on solute dipole moment. Neither was there any evidence that the polar/nonpolar domain formation in the higher homologs of the $[C_nC_1Pyr][NTf_2]$ series or in $[P_{6,6,6,14}][NTf_2]$ influences diffusion of solutes as small as benzene. Through Stokes-Einstein predictions, it was possible to observe that self-diffusion in ILs is like self-diffusion in conventional solvents. However, the relation to solute/solvent size ratio was greater in ILs than in conventional solvents [10].

2.2 Substituted aromatic molecules

2.2.1 Polyphenols (Catechins)

Barrulas et al. gave an important contribution for the NMR study of interactions between ILs and small molecules [20]. The articles so far were not very complete in terms of the NMR experiments available, lacking always some proof of concept. Extracts from plants like matcha green tea have considerable significance as bioactive compounds with several pharmacological applications, namely polyphenols (being catechins the most prevalent). Nonetheless, the amount of these compounds in the extracts is typically very low. Consequently, green extraction techniques with higher efficiency for phenolic compounds are of paramount importance, in which ILs can be used as designer solvents. In order to rationalize the interactions, several model compounds were selected – naphthalene to study π-π stacking, veratrole, L-3,4-dihydroxyphenylalanine (L-DOPA) to understand the behavior of the phenol moiety toward H-bonds and hydrophobic interactions, and 1,2-dihydroxyanthraquinone (alizarin) in order to study all the interactions simultaneously. Several ILs were tested: $[C_4C_1Im]Cl$, $[BzC_1Im]Cl$, $[C_2C_1Im]Cl$, $[C_4C_1C_1Im]Cl$, $[C_2C_1Im][OTf]$, $[C_2C_1Im][TCM]$, $[C_2C_1Im][DCA]$, and $[C_4C_1Im][OTf]$. The solutions resulting from the mixture of the ILs and the model compounds were tested through ^{1}H-DOSY and ^{1}H,^{1}H-NOESY NMR experiments (**Figure 3**). Both the IL cation and anion had an influence on the solvent behavior.

The best ILs for extracting matcha polyphenols were imidazolium derivatives with shorter alkyl sidechains and weakly basic anions such as $[TCM]^-$, $[DCA]^-$, and $[OTf]^-$. Finally, it was possible to locate π-π stacking and hydrophobic interactions in case of the cation and H-bond acceptor interactions in case of the anion [20].

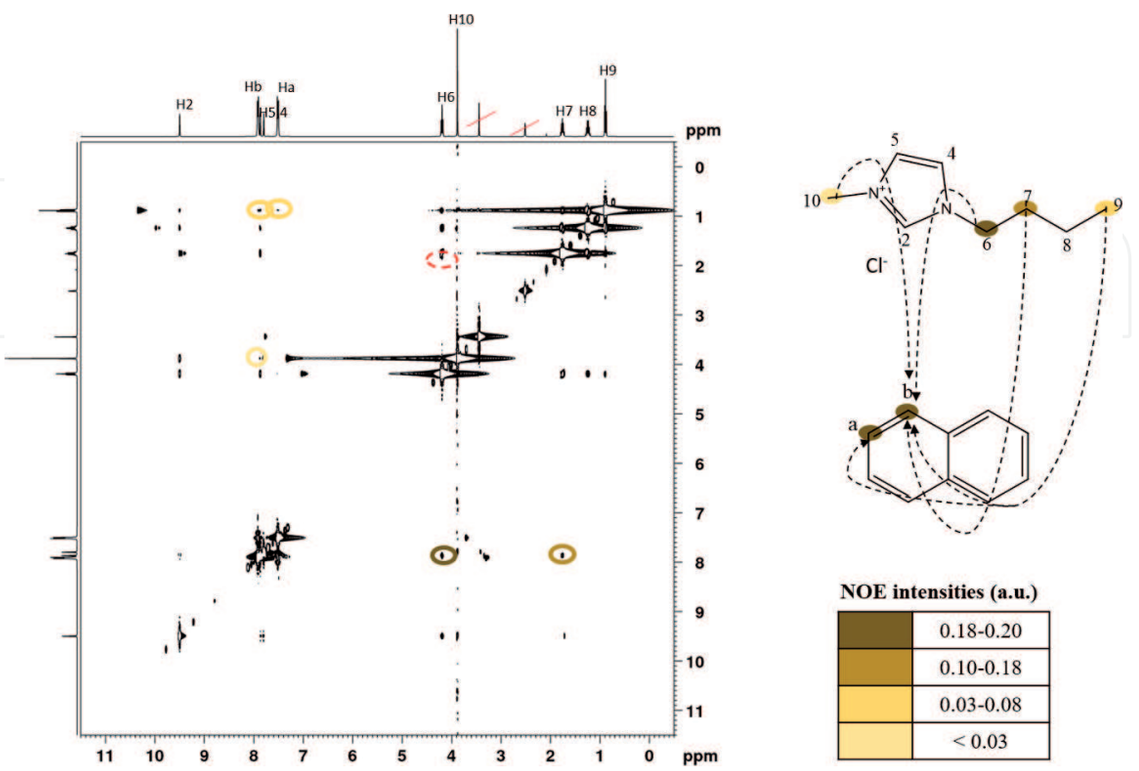

Figure 3.
2D ^{1}H,^{1}H-NOESY spectrum with 200 ms mixing time of $[C_4C_1Im]Cl$/naphthalene mixture [0.16:0.16 (M/M) in DMSO-d_6] and main intermolecular interactions (adapted from Ref. [20]).

2.2.2 5-Hydroxymethylfurfural

Nowadays, searching for new sources of green energy is crucial. Biomass is receiving attention, since the reserves are abundant, the price is low and is renewable. The preparation of 5-hydroxymethylfurfural (5-HMF) from biomass is a very interesting topic, since this compound is applied in the production of high value-added chemicals and biofuels [5, 21]. Thus, new high-efficiency reaction medium for the preparation of 5-HMF is needed, and ILs are suitable alternatives. Mixtures of 5-HMF and ILs with anion $[NO_3]^-$ and different cations $[C_4C_1Im]^+$, $[C_4Py]^+$, $[C_4C_1Pyr]^+$, $[C_nC_1Pip]^+$, and $[N_{1,1,1,H}]^+$ were studied and presented strong intermolecular interactions. In order to unveil the chemical nature of such interactions, ^{1}H NMR experiments were done for different ILs/5-HMF systems, and the $\Delta\delta$ of each proton was estimated [5]. In $[C_4Py][NO_3]$, the H-bond between the anion and the cation was mainly formed by O atom in $[NO_3]^-$ and H_2, H_5 atoms that were close to the N atom of the pyridine ring [5, 22]. Therefore, the upfield movement of H_2 and H_5 protons indicated that the input of 5-HMF into ILs weakens the H-bonding between anion and cation. With the addition of 5-HMF into ILs, the π-π interactions between pyridine rings became weaker and the shielding effect was strengthened, causing the protons of the alkyl chain in cation upfield shift. Based on ^{1}H,^{1}H-NOESY experiments, it was seen that the addition of 5-HMF induced the change of alkyl chain conformations, from gauche to trans. With the exception of $[C_4C_1Pyr]^+$ and $[C_nC_1Pip]^+$, $[C_4C_1Im]^+$, $[C_4Py]^+$, and $[N_{1,1,1,H}]^+$ could form H-bonds with hydroxyl group in 5-HMF, and this capacity increased as follows: $[C_4Py]^+ \approx [C_4C_1Im]^+ < [N_{1,1,1,H}]^+$. 5-HMF could strongly bind IL anions, while the H-bond interaction of 5-HMF with the cation was much weaker. Also, the interactions between the carbonyl group of 5-HMF and the cation of ILs were also very weak. Therefore, the cation impacted the interaction of 5-HMF with ILs through its interaction with the anion [5].

2.2.3 Fluorinated derivatives of benzene

Dias et al. studied the interactions between mixtures of $[C_2C_1Im][NTf_2]$ with benzene (discussed in Subsection 2.1), fluorobenzene, 1,2-difluorobenzene, 1,4-difluorobenzene, 1,3,5-trifluorobenzene, 1,2,4,5-tetrafluorobenzene, pentafluorobenzene, and hexafluorobenzene through 1D ^{1}H NMR and ^{13}C NMR and 2D ^{1}H,^{1}H-NOESY NMR spectroscopy [17]. Relative to ^{1}H NMR, it is important to highlight that proton H_2 was the most interactive site (most acidic proton) of the imidazolium cation, which means that any perturbation in the polar network of the IL was felt at this position. In case of the benzene mixtures, the aromatic protons exhibited larger shielding shifts than their aliphatic counterparts; thus, in case of $[C_2C_1Im][NTf_2]$/1,2-difluorobenzene mixtures, the H_2 protons exhibited small shielding shifts as the aromatic molecule concentration increased. At higher concentrations, these turned into small deshielding shifts. The aliphatic protons showed intermediate shielding shifts, and the H_4/H_5 protons displayed the largest shielding shifts. In case of $[C_2C_1Im][NTf_2]$/hexafluorobenzene mixtures, most shifts were deshielding through the order of $H_2 > H_6–H_8 > H_4/H_5$. When the aromatic molecules are interspersed in the polar network of the IL, there is a competition between the interactions with the oxygen atoms of the $[NTf_2]^-$ anion (OBT) and the π electrons or fluorine atoms of the aromatic solute. The polar network was stronger at the H_2–OBT contacts than at the H_4/H_5–OBT contacts. This led to a higher proportion of H_4 and H_5 protons interacting with the solute molecules, relative to H_2 interactions. With ^{13}C NMR, it was possible to observe that the carbon atoms attached to hydrogen atoms experienced small shielding shifts in the benzene mixtures that changed to larger deshielding shifts in mixtures with more

fluorinated aromatic molecules. The carbon atoms linked to fluorine atoms experienced deshielding shifts in the hexafluorobenzene mixtures that became progressively larger shielding shifts in mixtures with less fluorinated aromatic molecules. 2D NOESY spectra of the equimolar mixtures of $[C_2C_1Im][NTf_2]$ with 1,4-difluorobenzene and pentafluorobenzene identified a cross-peak between the H_8 protons of the IL and the protons of the aromatic molecule. Summing up, in benzene, the cations are mainly located above and below the aromatic plane, experiencing the diamagnetic influence of the aromatic electrons. As the aromatic ring becomes much more fluorinated, the cations migrate to the equatorial plane of the aromatic molecule, to a region of milder paramagnetic effect.

3. Interactions between ionic liquids and CO_2

NMR spectroscopy allows the direct measurement of CO_2 solubility as well as the evaluation of intermolecular interactions and sorption mechanism [23, 24]. Since ILs exhibit the ability to tailor many of their physical and chemical properties, such as gas solubility, they have been extensively studied in CO_2 sorption. Different sorption mechanisms can be observed according to the site and the strength of CO_2/IL interaction. Therefore, according to the CO_2 sorption mechanism, the ILs can be divided into three main groups: physisorption, chemisorption, and water sorption (**Figure 4**).

In general, CO_2/anion interactions are preferential in comparison to CO_2/cations; therefore, the classification of ILs in these three groups is mainly based on the anion functional group and respective IL properties. Non-basic nucleophilic anions capture CO_2 through a noncovalent pathway, and these anions belong to the first group. Basic anions that can form covalent bonds with CO_2 molecule belong to the second and third groups. Besides the functional groups of the anions and the mechanism of sorption, the main difference between ILs of the second and third groups is the products that are formed, since the third group reacts with the water existing in the IL.

Furthermore, the pressure and temperature may also affect CO_2 solubilization. For lower pressure applications, the chemisorption is favored; meanwhile, increasing the pressure, physisorption becomes preferential. A smart selection of pressure and IL structure is essential to develop a higher CO_2-philic material. It is important to

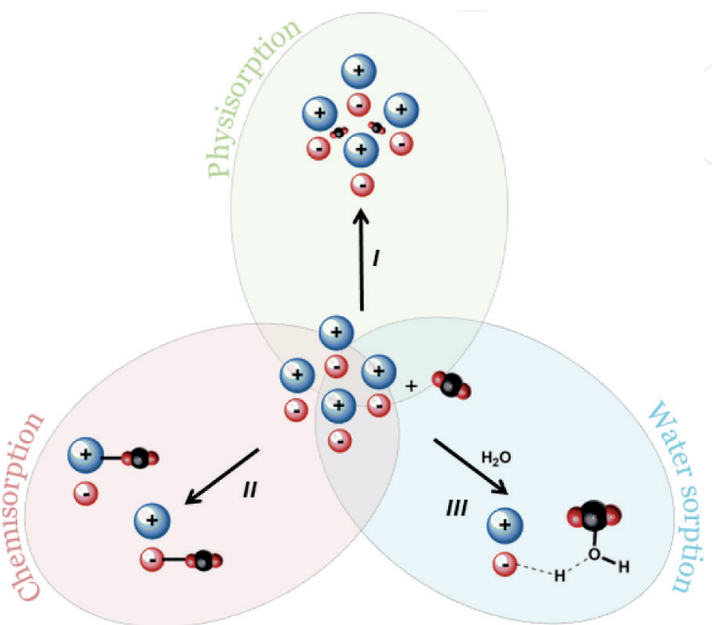

Figure 4.
Summary of CO_2-IL interactions observed by NMR experiments.

mention that all CO_2 capture mechanisms can occur simultaneously in a single IL. In this context, the NMR spectroscopy allows direct measurement of CO_2 solubility, intermolecular interactions, and sorption mechanism and performs *in situ* high pressure experiments. Therefore, the NMR is a powerful technique for designing ILs with high steric hindrance and low viscosity to capture CO_2 efficiently and selectively [23].

3.1 Noncovalent interactions—physisorption

To design an efficient sorbent for CO_2 capture, CO_2 transport properties need to be understood. In physisorption, the surface area of IL attracts CO_2 molecules by van der Waals forces. In this case, CO_2 sorption occurs mainly in ILs containing nonbasic-nucleophilic anions, like fluorinated anions. Based on 3D structures of ImILs that create ion cage-like structures with void spaces capable of confining CO_2, several NMR techniques were being used to study the capability of ImILs to absorb CO_2 and understand IL/CO_2 interactions.

Corvo and co-workers studied $[C_4C_1Im][PF_6]$, $[C_4C_1Im][BF_4]$, and other fluorinated ILs with slight changes in the aliphatic substituent as chain branching or elongation, such as $[(i\text{Pr})C_2C_1Im][NTf_2]$ and $[C_4C_1Im][NTf_2]$, respectively. The cation/anion, cation/cation, cation/CO_2, and anion/CO_2 interactions were analyzed through NOE, DOSY, and relaxation experiments, at 10 and 80 bar, combined with molecular dynamics (MD) simulations (**Figure 5**) [24, 25].

The comparison of ^{1}H-^{1}H NOE cross-peak intensity in the presence and absence of CO_2 showed the direct cation/cation interactions. Cross-peaks between the methyl group and the methylene of the aliphatic chain are particularly informative because they reflect only intercationic interactions. From the NOESY data for

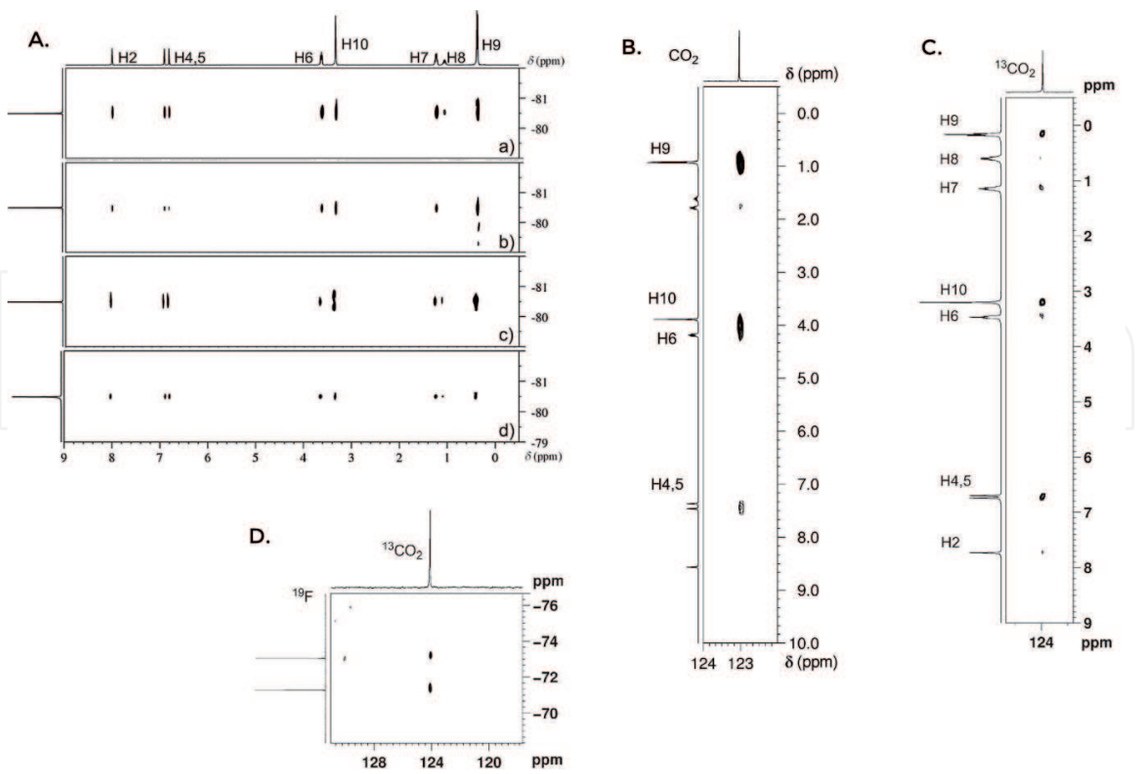

Figure 5.
(A) ^{1}H,^{19}F-HOESY spectra with 400 ms mixing time of $[(i\text{Pr})C_2C_1Im][NTf_2]$: (a) neat IL at 298 K; (b) mixed with 10 bar CO_2 at 298 K; (c) neat IL at 313 K; (d) mixed with 80 bar CO_2 at 313 K; (B) ^{13}C,^{1}H-HOESY spectrum of $[(i\text{Pr})C_4C_1Im][NTf_2]$, with 10 bar of $^{13}CO_2$ at 298 K; (C) ^{13}C ,^{1}H-HOESY spectra (500 ms mixing time) of $[C_4C_1Im][PF_6]$, mixed with $^{13}CO_2$ at 298 K and 11 bar; (D) ^{13}C,^{19}F-HOESY (400 ms mixing time) of $[C_4C_1Im][PF_6]$, mixed with $^{13}CO_2$ at 298 K and 11 bar (adapted from Refs. [24, 25]).

neat IL and IL/CO_2 solutions, it was possible to conclude that at 80 bar, the pattern of cation/cation interactions changes considerably with the correlations between protons of the methyl group H_{10} (NCH_3) and the sidechain protons $H_7/_8$ almost absent from the spectra.

^1H,^{19}F-HOESY experiments showed essentially the cation-anion contacts. Due to the geometry of the anion, the $[NTf_2]^-$ in ImIL was near to the terminal methyl groups (RCH_3 and NCH_3) in linear and branched chain. After CO_2 dissolution, the similarity on the cross-peak intensity from the ^1H,^{19}F-HOESY experiment indicated that the cation/anion contacts were mostly the same as in the neat ILs (**Figure 5a**). The main differences between the neat ILs and the IL/CO_2 mixtures indicated the locations that were mostly affected by CO_2 solvation. At 10 bar of CO_2, the aromatic protons H_4/H_5 presented stronger correlations with the anion and also the methyl group NCH_3. At 80 bar of CO_2, the fluorine contacts with the nonpolar domains, specifically with the methylene protons and the methyl groups, decrease slightly. As **Figure 5b** demonstrates, in the ^{13}C,^1H-HOESY spectra of $[(i\text{Pr})C_2C_1\text{Im}][NTf_2]/CO_2$ mixture, CO_2 was located around the methyl group RCH_3 and the isopropyl methyl group, proving the direct cation-CO_2 interactions. The HOESY experiments also indicate that increasing CO_2 pressure may lead to the deformation of the ion cage structure of the ILs, accommodating more CO_2 molecules.

^{13}C,^1H-HOESY and ^{13}C,^{19}F-HOESY experiments proved cation-CO_2 and anion-CO_2 interactions. Analyzing the ^{13}C, ^1H-HOESY spectra from the $[C_4C_1\text{Im}][PF_6]$, at 10 bar using ^{13}C-labeled CO_2 was possible to notice strong interactions between CO_2 and the aromatic protons H_4/H_5, the methyl group RCH_3 of alkyl chain and the methyl protons of NCH_3 (**Figures 5b**, **c**). In the same way, the ^{13}C,^{19}F-HOESY experiment confirmed the existence of direct anion-CO_2 interaction (**Figure 5d**).

By using ^{13}C-T_1 NMR relaxation experiments, it was possible to conclude that at low pressure, the solubilization of CO_2 has a minimum effect in the global mobility of the IL. Meanwhile, the opposite was observed for higher pressure (80 bar). Taking into consideration all the experimental data, it was possible to conclude that the physisorption of CO_2 occurs in the cavities near methyl groups NCH_3 and RCH_3 and aromatic protons H_4/H_5 [24, 25].

Taking advantage of known physical sorption of CO_2 in $[C_4C_1\text{Im}][NTf_2]$, Allen and Damodaran had chosen this IL to evaluate the diffusion of CO_2 in ILs. Slice-selective inverse gated pulse field gradient technique was employed and demonstrated as an excellent alternative to study gas dynamic solvation under non-equilibrium conditions in a method similar to magnetic resonance imaging (MRI) [26].

3.2 Covalent bond—chemisorption

Many ILs have previously been reported as physical sorbents for CO_2, under different pressures. More recent studies described the capability of ILs to interact through a chemical pathway with CO_2, under low pressures. ILs that contain reactive functional groups, usually N or O moieties on the cation or the anion, can bond covalently with CO_2, which results on the formation of carbamates or carboxylates, respectively. 1D and 2D NMR techniques can easily prove the chemical CO_2-IL interactions.

3.2.1 Carboxylates

Due to the possibility of chemical sorption between CO_2 and the 2-position of the imidazolium ring, ImILs with carboxylate anions have been intensely studied. In 2012, through the ^{13}C NMR analysis, the chemical reaction and the formation of 1,3-dialkylimidazolium-2-carboxylate and acetic acid were reported for the

first time, by Blath and co-workers and Danten and co-workers. Both proposed a mechanism of the CO_2 absorption [27–29].

Danten and co-workers started their study with the comparison between the ^{13}C NMR spectra of the pure IL with the CO_2-IL mixture and observed a new signal ca. 155 ppm connected with the CO_2.

The comparison of the ^{15}N NMR spectra of the pure IL with the IL/CO_2 mixture proved the carboxylation into imidazolium ring by the observation of two intense signals at 183.7 and 171.6 ppm assigned to the nitrogen atoms of the ring core. In the mixture, two additional resonance signals flanking each of the previous peaks were observed at 182.1 and 170.0 ppm, respectively (**Figure 6a**). The 2D $^{1}H,^{15}N$-HMBC spectra of the mixture proved the correlation between the new signals and the secondary peak observed in the ^{1}H NMR spectrum of the IL/CO_2 mixture (**Figure 6b**).

To understand the favored chemical site among the three possibilities (C_4/C_5 and C_2), the 2D spectrum using the INADEQUATE sequence was performed. The C_2 signal of the $[C_4C_1Im]^+$ cation (138.3 ppm) was not correlated with the two new peaks located at 155.3 and 141.6 ppm (**Figure 6d**). These two peaks were correlated showing the formation of a new species in which CO_2 is covalently bonded to the C_2 of the imidazolium ring (**Figure 6c**) [28, 29].

Another similar study lead by Kortunov, employing non-aqueous $[C_2C_1Im][OAc]$, supported these conclusions. Once again, the presence of the signal at 155.3 ppm in the ^{13}C NMR spectrum indicated the presence of the carboxylate complex. To reinforce this idea, the $^{1}H,^{13}C$-HSQC and ^{13}C DEPT-135 NMR experiments were executed, neither the new carbon peaks (141.5 and 155.1 ppm) have protons directly attached nor the new proton signal (15.7 ppm) has any carbon attached [30].

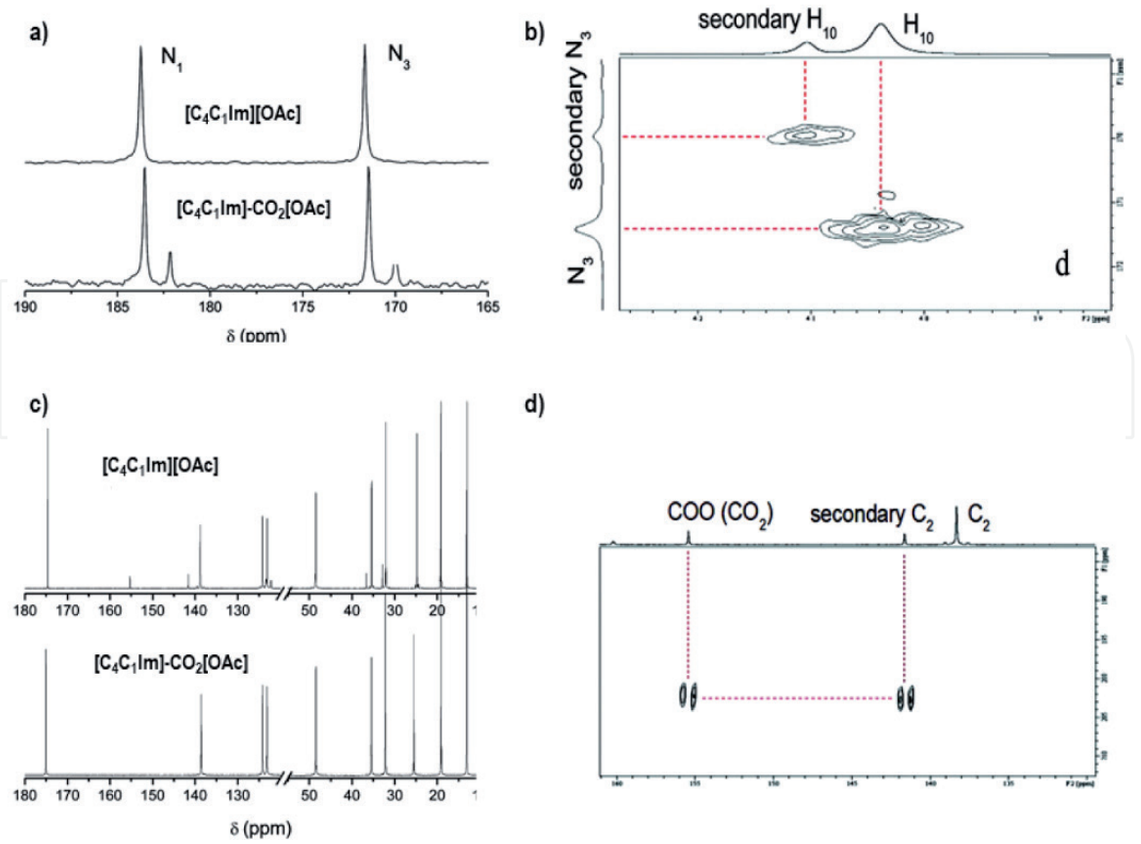

Figure 6.
(a) ^{15}N NMR spectra of the neat $[C_4C_1Im][OAc]$ and $[C_4C_1Im][OAc]/CO_2$ mixture; (b) correlation in $^{1}H,^{15}N$-HMBC of $[C_4C_1Im][OAc]/CO_2$ mixture; (c) ^{13}C NMR spectra of the neat $[C_4C_1Im][OAc]$ and $[C_4C_1Im][OAc]/CO_2$ mixture; (d) ^{13}C NMR INADEQUATE of $[C_4C_1Im][OAc]/CO_2$ mixture (adapted from Ref. [28]).

Other essential work using carboxylate anions has been published by Umecky and co-workers. The authors prepared task-specific ImILs with 2,4-pentanedionate and fluorine derivatives to use as CO_2 chemical absorbents. The experiments were performed in neat IL and in dichloromethane solution (50 vol%) by bubbling CO_2. A comparison of ^{1}H NMR spectra among the fluorinated and carboxylate anions showed that the acidity of the hydrogen atom at the 2-position strongly influences the CO_2 sorption capacity. The chemisorption of CO_2 is governed not only by the anion basicity but also by the acidity of H_2 and the possibility of its abstraction. By using 2D analysis (HMQC and HMBC), it was possible to prove the formation of a complex between $[C_2C_1Im]^+$ and CO_2. In those conditions, the influence of dissolved water and consequently the formations of the carbonate (CO_3^{2-}) and bicarbonate (HCO_3^-) were negligible [31].

Ether-functionalized ImILs were also capable of capturing the CO_2 physically and chemically. The physisorption was proved by Seo et al. and the chemisorption by Sharma et al. Both studies were accomplished through ^{13}C NMR and FTIR techniques. Sharma et al. proposed a mechanism for the formation of the carboxylic acid based on ca. 205 ppm signal in the ^{13}C NMR [32, 33].

3.2.2 Amines

The use of ILs containing a basic amine group (task-specific ILs) to capture CO_2 by chemical reactions was reported for the first time by Davis group [34]. After that, amine-based ILs have been the focus of many works, due to their highly efficient capacity on gas solubilization. Generally, the aqueous solution of primary and secondary amines reacts with CO_2 yielding carbamates. On the other side, the reaction between CO_2 and the tertiary amine depends on water amount in the system. The formation of carbamate and bicarbonate has been demonstrated; however, the reaction is still a critical point of discussion and merits further investigations [35, 36].

Combining the idea of low toxicity and high reactivity toward CO_2, a series of choline-based amino acid ILs were reported by Bhattacharyya and Shah. DFT calculations, IR, and NMR spectroscopic techniques were employed to examine the mechanism of the CO_2 interaction with ILs. The ^{1}H, ^{13}C, and ^{1}H,^{1}H-COSY NMR analysis of $[N_{1,1,6,2O4}][Lys]$ demonstrated the signals shifted during the sorption procedure. In ^{13}C NMR spectrum, three new signals were observed: ca. 178 ppm attributed to carboxylate anion with a strong intermolecular hydrogen bonding; at 160.9 and 163.7 ppm attributed to the formation of carbamic acid and carbamate anion, respectively [37].

The CO_2 dissolution and the ionic mobility by diffusion experiments of choline-based ILs $[N_{1,1,6,2O4}]^+$ with $[Threo]^-$ and $[Im]^-$ anions were investigated by the same group. Once again, the formation of carbamic acid and carbamate anion ($[Threo]–CO_2$) was observed after CO_2 capture, by the presence of characteristic peaks (160.4 and 164.0 ppm) in ^{13}C NMR spectrum. In addition, the $[Threo]^-$ alpha proton represented by a doublet at 3.11 ppm shifted to 3.43 ppm, whereas the beta protons at 3.94 ppm shifted to 4.16 ppm and the methyl proton from 1.20 to 1.29 ppm after CO_2 reaction. By contrast, the ^{1}H NMR spectrum of $[N_{1,1,6,2O4}][Im]$ did not show significant $\Delta\delta$ after CO_2 absorption. However, in the ^{13}C NMR spectrum, a new signal at 160.8 ppm was observed and attributed to the formation of a carbamate specie. Both neat ILs demonstrated broadened signals in ^{1}H NMR spectra, particularly after CO_2 absorption. Using the diffusion decays of the stimulated spin echo, it was possible to observe that the diffusion of anion and cation was not affected by CO_2. The diffusion behavior of both ILs before and after absorbed CO_2 was also studied in a temperature range of 20–90°C. The diffusion of cations and anions changes by the same factor regardless of temperature. From the observed

^{1}H diffusometry results, the mobility increased for $[Im]^-$ IL after CO_2 sorption and decreased for $[Threo]^-$ anion. The authors explained this behavior based on the decrease in the aromaticity and electron density volume of the imidazolate by the formation of carbamate due to CO_2 reaction [38].

Over the last few years, NMR techniques have proven that the reaction between CO_2 and 1,3-dialkyl imidazolium cation is strongly dependent on the anion [27]. Chen et al. demonstrated that some functionalized ILs can interact physical and chemically with CO_2, by studying the behavior of $[aC_2C_1C_1Im][BF_4]$ with this gas. After CO_2 capture, the ^{1}H NMR spectrum showed duplicate signals and the ^{13}C NMR spectrum showed two new peaks, proving that part of $[aC_2C_1C_1Im][BF_4]$ interacts with CO_2 chemically, producing carbamic acid IL-NHCOOH (ca. 163 ppm), and the remaining $[aC_2C_1C_1Im][BF_4]$ interacts with CO_2 physically (ca. 160 ppm) [39].

More recently, the influence of CO_2 sorption in ion mobility in aqueous solution (50/50 wt%) of similar choline-based amino acid ILs was evaluated by Filippov et al. Similar to their previous work, they proposed a mechanism of CO_2 sorption in IL containing amino acid anion (such as $[Threo]^-$) process by carbamic acid and carbamate anion formation, proved by the presence of the signal ca. 159 ppm. While the water diffusivity was not affected by the absorption of CO_2, the increase in ion mobility upon CO_2 chemisorption was demonstrated by employing ^{1}H and ^{13}C NMR diffusion experiments [40].

Brennecke's group prepared a series of alkyl-phosphonium cation ILs with aprotic heterocyclic anions (AHAs) and studied the CO_2 capture in dry and wet conditions. All anions correspond to a tertiary amine incorporated into a heterocyclic ring: indazolide, imidazolide, pyrrolide, pyrazolide, and triazolide-based anions. In dry conditions, they suggested a formation of carbamate species, via Lewis acid-base interaction. Comparing the ^{1}H NMR chemical shifts of the dry with wet protonated-heterocyclic anions, they concluded that the $[P_{6,6,6,14}][2\text{-CNPyr}]$ did not suffer from the anion reprotonation in the presence of water and CO_2, and the opposite trend was previously reported by them for $[P_{6,6,6,14}][Pro]$. In that case, due to reprotonation and deactivation of the anion, the water reduced the CO_2 molar capacity. Even though they did not discard the bicarbonate formation from CO_2 and water, they believed that the amount of bicarbonate formed was not expected to be prevalent enough at such low CO_2 pressure. For the $[P_{6,6,6,14}][2\text{-CNPyr}]$, the addition of 5 wt% of water increased the CO_2 solubility, and the authors suggested a change in the IL-CO_2 complex activity upon water addition. However, no ^{13}C NMR spectra have been reported to confirm the theory [41, 42].

Based on the concept of preorganization, a novel CO_2 sorption mechanism using $[P_{4,4,4,2}][Suc]$ was addressed by Huang et al. Through a combination of ^{13}C NMR, FTIR, and quantum chemical calculations, they suggested an innovative structure organization with superior CO_2 capacity resulting from the interaction between CO_2 and the $[Suc]^-$ anion [43]. Following this idea, the authors also published the tuning of those imide-based anion IL with phosphonium cations by the addition of the electron-donating group. By changing the CO_2 sorption amount, several ^{1}H NMR and ^{13}C NMR spectra were acquired, and the cooperative interactions between anion and CO_2 were reinforced. According to the authors, at the first stage, the absorption was dominated by N-CO_2 interaction confirmed by the presence of a new signal ca. 159 ppm and by the shift of the signal from 195.6 to 188.0 ppm related to C═O anions. The second stage of absorption mechanism was dominated by the additional O-CO_2 interactions, as suggested by the shift of the same signal to 182.8 ppm. The physical interaction occurred at the last stage and is weaker than the first two. This was confirmed by ^{1}H NMR spectrum through the shift of the signal from 1.23 to 1.30 ppm during the uptake of CO_2, that indicates the physical hydrogen bond between methylene in the anion and oxygen atom of the CO_2 (C-H-O) [44].

3.3 CO_2 interaction in wet ionic liquids

Since most ILs are hygroscopic, dry ILs are extremely difficult to obtain. The presence of water in ILs can affect many properties, including CO_2 sorption. In this field, a few groups started to evaluate the CO_2 capture in wet ILs. Using analogous phosphonium-based ILs and experimental conditions, our group has demonstrated a different point of view of Huang et al. based on NMR analysis. Combining the ^{13}C-$\{^1H\}$, attached proton test (APT), phase-sensitive HSQC, HMBC, and ^{31}P-$\{^1H\}$ NMR spectra, the degradation of $[Suc]^-$ anion was proposed. The ^{13}C-$\{^1H\}$ NMR spectra showed a second set of signals that did not correspond to the $[P_{4,4,4,2}]^+$ or $[Suc]^-$ at 34.4, 35.4, 174.8, and 176.4 ppm. Those signals were observed at APT analysis and represent two CH_2 groups and two C═O, indicating IL degradation or contamination. Combined with the correlation between protons and carbons observed by HMBC and HSQC experiments, the analysis suggested the formation of 4-amino-4-oxobutanoate (anion from succinamic acid) resulting from the basic hydrolysis of the pyrrolidine-2,5-dione (SucH) during the synthesis of IL. Furthermore, the formation of bicarbonate by the reaction between CO_2 and IL confined water was proposed due to the presence of the signal ca. 159 ppm. The same chemical shift was observed for $[P_{4,4,4,2}][HCO_3]$ IL, reinforcing the idea of bicarbonate formation [45].

Davis and co-workers demonstrated that the CO_2 capture is hugely impacted by the presence of water in a series of $[N_{1,1,1,1}]$ ILs having amino acid anions. Employing ^1H and ^{13}C NMR analysis, they demonstrated the formation of a carbamate only as transitory specie (ca. 163 ppm) for amino acid ILs. Indeed, when the amount of CO_2 present in the system exceeds about 0.5 mol/mol of IL present, the carbamate complex was detected in trace amounts and the carbonate/bicarbonate capture emerged as predominant. Due to rapid proton exchange, carbonate and bicarbonate appear as a single peak ca. 159 ppm. The study also reported the CO_2 sequestration in wet $[N_{1,1,1,1}][2\text{-CNPyr}]$; in the ^{13}C NMR spectrum, the migration correlated with proton sequestration, and the carbonate/bicarbonate peak was observed; however, the signal associated with carbamate formation was not observed, in opposition of Brennecke's work [41, 42, 46].

Recently, Filippov et al. using solid-state ^{13}C and ^{15}N MAS NMR spectroscopy demonstrated the CO_2 absorption in $[N_{1,1,n,2OH}][Threo]$ and $[N_{1,1,n,2OH}][Tau]$ aqueous solution (50 wt%) ILs. After CO_2 reaction, a precipitated product appeared and was analyzed by ssNMR (^{13}C and ^{15}N), suggesting that the solid sediment is composed of neutral threonine (or taurine) in the zwitterionic forms. Therefore, they assigned the resonance line at 164.4 ppm to the formation of the carbamate anion and the resonance line at 160.6 ppm to the carbamic acid [47].

The confinement of a water molecule between the cation and the anion in ImILs was demonstrated through NOESY experiment by our research group. This water can react reversibly with CO_2 to yield bicarbonate. The phenomenon occurred only with basic anions, such as $[OAc]^-$ and $[Im]^-$. Whereas fluorinated anions, such as $[BF_4]^-$ and $[NTf_2]^-$, show only noncovalent interactions with CO_2, and no significant contacts between water and cation could be detected. In the same work, ^{13}C inverse-gated decoupled analysis was employed to quantify the CO_2 capture by an aqueous solution of $[C_4C_1C_1Im][Im]$ and $[C_4C_1C_1Im][OAc]$. The best system $[C_4C_1C_1Im][Im]/H_2O$ (1/1000) presented a sorption capacity of 10 molCO_2/molIL. Additionally, the comparison between the ^1H,^{15}N-HMBC NMR spectra of $[C_4C_1C_1Im][Im]/D_2O$ (1/1000) neat and under 20 bar of CO_2 reinforced the idea of bicarbonate formation instead of carbamate, since it was not observed any change in the chemical shift [48].

The formation of bicarbonate was demonstrated, once again, by Dupont and co-workers for bare ImILs under 10 bar of CO_2. In this work, the water in the

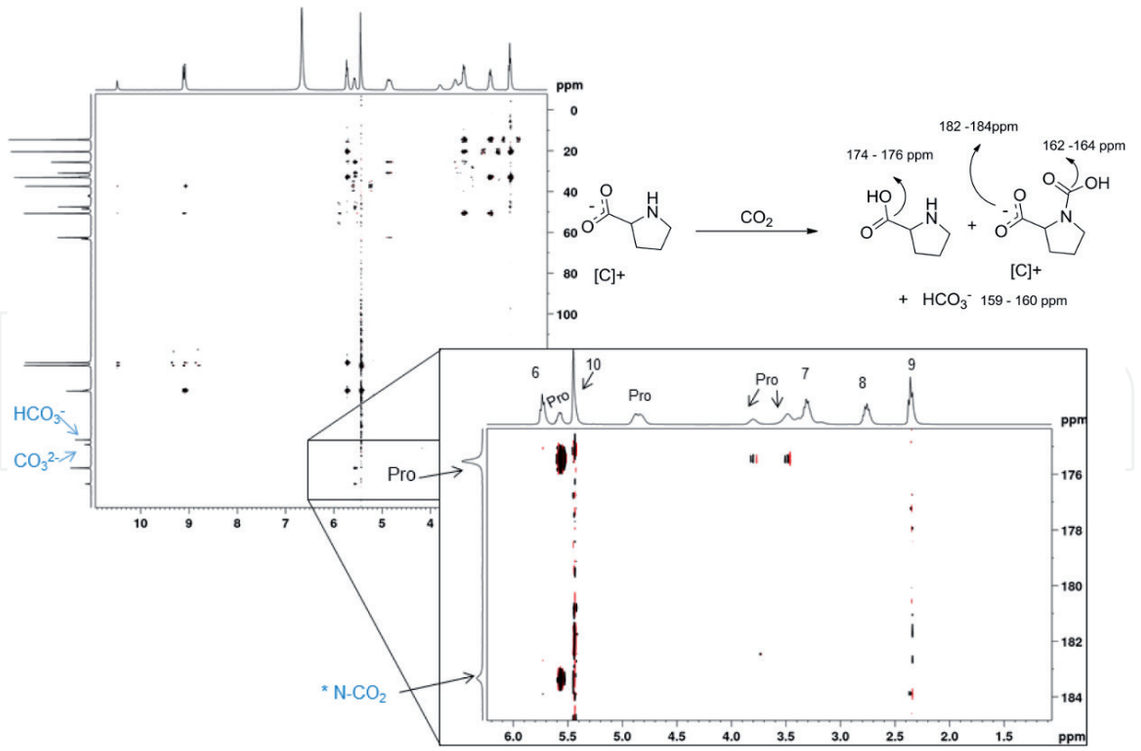

Figure 7.
Possible reaction of $[C_4C_1Im][Pro]$ after bubbling CO_2 and $^1H,^{13}C$-HMBC NMR experiment (100 MHz, DMSO-d_6 capillary) (adapted from Ref. [49]).

hygroscopic IL was enough for the signal related to HCO_3^-/CO_3^{2-} species (ca. 160 ppm) to appear in ^{13}C NMR. A description of interactions between ImIL and CO_2 was demonstrated combining NMR spectroscopy with MD simulation. According to the ImIL structure, three types of CO_2-IL interaction were described: physical sorption by the polar domains (halogenated anions); chemical sorption by reaction with cation and formation of $[C_4C_1Im]$-CO_2 complex or by reaction with anion by carbamate formation (amino acid anions); and bicarbonate formation (hygroscopic basic anions). Another interesting result to point out in this work is $[C_4C_1Im][Pro]$-CO_2 interaction. Through the contour map of $^1H,^{13}C$-HMBC associated with ^{13}C NMR studies, it was possible to understand the CO_2 sorption mechanism and observe the pH dependence for this anion. Bubbling CO_2 in neat IL, the ^{13}C NMR signals suggested a reaction with the $[Pro]^-$ anion and the formation of the carbamate (ca. 180 and 162 ppm) and bicarbonate (ca. 161 ppm), which was confirmed by $^1H,^{13}C$-HMBC (**Figure 7**). This work demonstrated that the sorption capacities of ImILs could be enhanced by the variation of cation-anion-CO_2 and IL-CO_2-water interaction, providing a helpful investigation to understand the structure-activity relation in IL materials for CO_2 capture [49].

4. Interactions between ionic liquids and cellulose

Cellulose is a natural, renewable, and the most abundant polymer in nature [50]. The applications range from the papermaking industry and film manufacturing to pharmaceuticals. Cellulose's poor solubility in common solvents is attributed to inter and intramolecular H-bonds, which limits its uses and imposes very harsh treatments like the Lyocell process (N-methylmorpholine N-oxide dissolution) and solvent systems such as LiOH/urea, dimethyl sulfoxide (DMSO)/$[N_{4,4,4,4}]F$, and dimethylacetamide (DMAc)/LiCl.

ILs have been used successfully to dissolve cellulose either using pure ILs such as $[C_4C_1Im]Cl$ and $[C_4C_1Im][OAc]$ or using binary mixtures with organic solvents such as DMSO.

Although there are several strategies to dissolve this polymer, the dissolution process is still poorly understood. Alkali salts like LiOH or NaOH mixtures with urea are one of the most employed solvent systems. The dissolution and gelation of cellulose in 8 wt % $NaOH/H_2O$ with and without the addition of urea were studied using polarization transfer NMR techniques (PTNMR), INEPT, and CP [51]. It was revealed that the solvent containing urea is able to fully dissolve cellulose. The use of liquid state polarization technique (INEPT) and a solid-state polarization technique (CP) allowed the discrimination of liquid and solid states. It was noted by the authors that the presence of some signal in the fully dissolved urea/$NaOH/H_2O$ solution is due to the reorientation dynamics of a very viscous sample, leading to some CP transfer.

The dissolution of cellulose in LiOH/urea was studied using solid-state NMR (ssNMR), by using ^{13}C CP/MAS NMR, ^{6}Li CP/MAS NMR, ^{6}Li single-pulse NMR, 2D heteronuclear $^{1}H,^{13}C$, and $^{1}H,^{6}Li$-(FSLG-HETCOR) [52]. Four existing forms of Li^+ ions were detected. Some Li^+ ions coordinate with cellulose chain, and a large population of Li^+ ions in the form of Li^+-OH^--urea surrounds the Li^+-cellulose chains, which prevent their self-aggregation. The ability to dissolve cellulose is likely determined by the coordination ability of alkali metal ions (Li^+, Na^+, K^+).

XRD and NMR methods were used to study the low-temperature dissolving mechanism of chitin/chitosan in the alkali (LiOH, NaOH, and KOH) aqueous solvents [53]. Aqueous alkali showed different dissolving abilities based on the acetylation degree (AD) of chitin, namely, KOH > NaOH >> LiOH for AD between 0.94 and 0.74; KOH ≈ LiOH ≈ NaOH for AD between 0.53 and 0.25; and the inverse order, LiOH > > KOH > NaOH for AD lower than 0.25. By measuring the active species of cations in semi-frozen solutions using ^{7}Li, ^{23}N, and ^{39}K NMR, differences from the stoichiometric quantities were obtained with a Na^+/Li^+ ratio higher than K^+/Li^+, which is the proposed explanation to the sodium higher destabilizing effect of chitosan at lower temperatures.

$[C_nC_1Im][(C_1O)PHO_2]$ was used to dissolve and regenerate cellulose under mild conditions [54]. Requiring heating to 80°C and being able to dissolve up to 4 wt%, coagulation with water afforded cellulose as a transparent gel. NMR was used to monitor the dissolution process by measuring ^{31}P and ^{13}C chemical shift differences to the pure IL. PLM photographs show complete dissolution after 120 min of heating.

Minnick et al. studied the solubility of cellulose in mixtures of $[C_2C_1Im][(C_2O)_2PO_2]$ with aprotic solvents (DMSO, dimethylformamide, 1,3-dimethyl-2-imidazolidinone) and protic antisolvents (water, methanol, and ethanol), concluding that polar aprotic solvents/IL mixtures can improve the cellulose solubility, while polar solvents have the opposite effect [55]. The ^{1}H $\Delta\delta$ of the IL-cation imidazolium ring resonances presented downfield shifts for the aprotic solvents, while protic solvents have the opposite effect. The reduced shielding experienced by the IL in aprotic solvents can be attributed to the solvation of the cation, which decreases cation-anion interactions, resulting in an increase in anion availability to form more and stronger interactions with cellulose. The authors explained negative chemical shift variations of IL in protic solvents as a result of stronger IL-solvent interactions, which change/compete with the IL-cellulose interactions.

On the use of an organic solvent as co-solvent of cellulose, DMSO was used in conjunction with $[C_nC_1Im]Cl$ to dissolve cellulose, using NMR relaxation measurements to study the dissolution process and co-solvation ability of DMSO [56]. At low concentration, DMSO improves the cellulose solvating ability of $[C_nC_1Im]Cl$ by reducing the viscosity of the IL but weakens it at high concentration.

T_2 measurements on ^1H and 1D spectra on ^1H, ^{35}Cl indicate that the tight association between the cation and the anion in the $[C_nC_1Im]Cl$ network is loosened at low DMSO concentration. Neat $[C_nC_1Im]Cl$ exhibits one population with smaller T_2 having a slower rotational dynamics and another with a larger T_2 and faster rotational dynamics. When DMSO concentration was increased, the $[C_nC_1Im]Cl$ with slower rotational dynamics transfers to faster rotational dynamics by going through a coalescence step at 0.4 DMSO molar fraction. Analysis of $\Delta\delta$ allowed probing the ion clustering, by studying the imidazolium H-bond change with DMSO addition and by using ^{35}Cl NMR to access the chlorine local environment. At 0.5 DMSO molar fraction, a turning point in ^{35}Cl NMR shifts is also observed, in a similar way as in T_2 relaxation. As imidazolium ^1H shifts change due to the shielding effect, the higher concentration of DMSO breaks the IL H-bond network into small ion clusters that are incapable of dissolving cellulose.

NMR PFG-diffusion was used to study the dissolving process of microcrystalline cellulose in aqueous tetrabutylammonium hydroxide $[N_{4,4,4,4}][OH]$ at 40 wt% concentration [57]. From the molecular self-diffusion coefficients of microcrystalline cellulose (MCC) and $[N_{4,4,4,4}][OH]$, $[N_{4,4,4,4}]^+$ is involved in the dissolution of carbohydrates, binding in a 1.2 stoichiometry to glucose units based on diffusion measurements and mass relations. The binding might be due to electrostatic interactions between the deprotonated hydroxyl groups or to hydrophobic effects, which have been discussed in the literature as important in cellulose dissolution by using either NMR or other techniques, such as calorimetry and rheology [58, 59].

Another use of cellulose is to make physical composites by blending it with another polymer to reinforce the final material. To understand the molecular origin of the enhanced mechanical properties for a cellulose/Silk blend film (SF), ssNMR was used as the tool to investigate the conformational changes, intermolecular interactions between cellulose and silk, and the water organization [60]. ssNMR can be used to gain an insight into polymer's molecular structure and dynamics, being able to identify its molecular constituents, structural morphology, and chain dynamics [61].

Cellulose/silk films were prepared by dissolution in $[C_4C_1Im]Cl$ followed by precipitation with methanol. 2D ^1H,^{13}C-HETCOR NMR reveals the intermolecular H-bonding interactions between the NH groups of SF and the OH groups bonded to carbons C_2 and C_3 of cellulose. 2D WISE experiments measured the hydrophilic character of each carbon sites, based on the lineshape with increasing mixing times, water is more localized in the vicinity of cellulose chains than silk.

5. Ionic liquids as co-solvents

ILs can be used as co-solvents in several applications, not only to increase the solubility of target species but also to tune the important physicochemical properties, such as conductivity and viscosity toward a more efficient industrial performance and operational conditions. In recent years, mixtures of ILs either with other ILs (IL/IL mixtures) [62, 63], molecular liquids (water, organic solvents) [64–66], or polymers [67] have gained such an interest that has been labeled as the fourth evolution of ILs [68]. IL mixtures do not fall in the definition of salt in solution, neither their physicochemical properties follow mixing behavior of molecular liquid mixtures, which create the need to develop new fundamental and structural/dynamic research.

In recent years, there has been an interest on mixtures of two or more ILs (IL/IL mixtures). This approach has been presented as a new strategy to tune the IL properties, with several studies showing that in most mixtures, physicochemical properties have close to ideal mixing behavior, due to a random ionic distribution (Coulombic interactions). However, non-ideal behavior has been reported, particularly for

mixtures with very different constituents [69, 70]. These "anomalies" can be explained by the formation of nano-segregated phases due to strong ionic interactions [71], making the ionic distribution nonrandom. Therefore, in terms of nanostructure organization, IL mixtures show an increased degree of complexity compared to neat ILs, having to consider the different combinations of the several ions present in solution. NMR techniques have been particularly useful to enlighten these deviations from linearity. Matthews et al. analyzed binary mixtures of ILs with a common cation $[C_4C_1Im]^+$ and different anions by ^1H and ^{13}C NMR chemical shift peak analysis [72]. Studying the full concentration range of IL/IL mixtures, they inferred that there is a preferential interaction of the cation with one of the anions. That was evident by the H_2 ^1H NMR peak, which shows a preferential interaction with the stronger H-bond acceptor anion over the NMR timescale. From the ^{13}C NMR, imidazolium ring C_4 and C_5 showed greater affinity for the weakest H-bond anions, which was not obvious in ^1H NMR, suggesting that the weakest H-bond will occupy a position above the plane of the imidazolium, forming an anion-π interaction. These slightly preferential associations have a very small effect on the structural organization but can be the driving force for nonideal deviations observed for some ILs.

Marullo et al. used $[BzC_4Im][NTf_2]$ with $[Bz(F_5)C_4Im][NTf_2]$ or $[BzC_4Im][BF_4]$ or $[N_{3,3,3,4}][NTf_2]$, as a function of the composition, as solvents for the Diels Alder reaction of 9-anthracenemethanol with N-ethylmaleimide [73]. The authors observed that the reactivity is affected by two main solvent parameters: the viscosity and the molecular organization. For IL/IL mixtures sharing the same cation, the kinetic rate was showed to be more affected by composition, correlating to structural modifications due to a more ordered local domain. For the anion shared IL/IL mixtures, they observed an unexpected result: changing the molar ratio of two cations with similar size and chemical nature produced a more profound effect on the reaction kinetics than IL mixtures ($[BzC_4Im]_x[N_{3,3,3,4}]_{1-x}[NTf_2]$) with different size cations. ^1H Δδ showed that the imidazolium H_2, H_9, and H_{10} exhibit a significant upfield shift, in which H_2 and H_9 show two chemical shift domains, with a discontinuity point, $[BzC_4Im]_{0.4}[N_{3,3,3,4}]_{0.6}[NTf_2]$, corresponds to the maximum rate, to which the authors justified with the transition point between a typical aliphatic IL and an aromatic type IL.

One of the applications of ILs is in the field of tribology [74]. ILs can be used as a lubricant by itself or as an additive to increase commercially available oil efficiency. Combining low molecular weight polyethylene glycol (PEG) with orthoborate ILs allowed a decrease in the wear and friction properties for steel on steel contacts. Filippov et al. studied mixtures of PEG 200 with ImILs derived from $[BMB]^-$ or $[BOB]^-$ anions as function of concentration by diffusion NMR and Δδ [75]. The chemical shift analysis showed that the presence of PEG affects the chemical shift of both the cations and the anions, with the protons of the imidazolium ring of the cation the most affected. For the anions, $[BMB]^-$ showed two chemical shift domains in the PEG concentration range, suggesting that above 50% wt PEG, there is a modification on the interaction mode of PEG/IL, which is not visible for the ImIL derived from $[BOB]^-$. The diffusion experiments showed that for ImIL derived from $[BMB]^-$, the cation and anion differ on their diffusion coefficient in all the concentration range, which suggested that in the mixture, the IL is partially dissociated, which agrees with the data obtained from impedance analysis.

6. Conclusions

The combination of different NMR experiments allowed to observe the molecular panorama of cation-anion-solute interactions. The diversity of NMR techniques at our disposal allows gathering crucial information to rationalize the IL solvent

behavior. Despite the notion that ILs are tailored solvents, their optimization is still seldom done on the basis of the fundamental knowledge of IL performance and the dissolution mechanisms. Instead, the trial and error approach often prevails.

The success of ILs as solvents depends on the strength and nature of the interactions that cations and anions can establish with the solute while maintaining their intrinsic interaction. Chemical shift deviation analyses identify the electronic perturbations in nuclei, either by making or breaking H-bonds or by inducing changes in the geometry. NOE experiments allow a more complete picture, probing solute structural organization within ILs; in this case, both strong and weak interactions can be identified. Relaxation studies are capable of sensing a shorter timescale and identifying even short-lived events that take place upon solubilization processes. Finally, diffusion studies in ILs provide the knowledge of solute behavior and respective associations and also cation/anion feedback in the presence of the solute. This information allows probing macroscopic properties, such as viscosity, which are intimately related to the desired application of ILs.

Acknowledgements

This work was funded by FCT—Portuguese Foundation for Science and Technology, Portugal, under the projects PTDC/EPH-PAT/0224/2014, PTDC/QUI-QFI/31508/2017, POR Lisboa, and PTNMR (ROTEIRO/0031/ 2013; PINFRA/22161/2016), co-financed by FEDER through COMPETE 2020, Portugal, POCI, and PORL and FCT through PIDDAC (POCI-01-0145-FEDER-007688; UID/CTM/50025/2019; and UID/Multi/04378/2019). T.G.P. acknowledges FCT for the SFRH/BD/133447/2017 PhD fellowship.

Conflict of interest

The authors declare no conflict of interest.

Abbreviations

Cations

$[(i\text{Pr})C_2C_1Im]^+$	1-methyl-3-isopentylimidazolium
$[aC_2C_1C_1Im]^+$	1,2-dimethyl-(3-aminoethyl)imidazolium
$[Bz(F_5)C_4Im]^+$	1-(2,3,4,5,6-pentafluorophenyl)-3-butylimidazolium
$[BzC_1Im]^+$	1-benzyl-3-methylimidazolium
$[BzC_4Im]^+$	1-benzyl-3-butylimidazolium
$[C_1C_1Im]^+$	1,3-dimethylimidazolium
$[C_2C_1Im]^+$	1-ethyl-3-methylimidazolium
$[C_4C_1C_1Im]^+$	1-butyl-2,3-dimethylimidazolium
$[C_4C_1Im]^+$	1-butyl-3-methylimidazolium
$[C_4C_1Pyr]^+$	1-butyl-1-methylpyrrolidinium
$[C_4Py]^+$	1-butylpyridinium
$[C_nC_1Im]^+$	1-alkyl-3-methylimidazolium
$[C_nC_1Pip]^+$	1-butyl-1-methylpiperidinium
$[C_nC_1Pyr]^+$, n = 3, 4, 6, 8, and 10	1-alkyl-1-methylpyrrolidinium
$[N_{1,1,1,1}]^+$	tetramethylammonium

$[N_{1,1,1,H}]^+$	trimethylammonium
$[N_{1,1,n,2OH}]^+$	alkyldimethyl(2-hydroxyethyl)ammonium
$[N_{3,3,3,4}]^+$	n-butyltriethylammonium
$[P_{4,4,4,2}]^+$	tri-n-butylethylphosphonium
$[P_{6,6,6,14}]^+$	trihexyl(tetradecyl)phosphonium

Anions

$[BF_4]^-$	tetrafluoroborate
$[BMB]^-$	bis(mandelato)borate
$[BOB]^-$	bis(oxalato)borate
$[2\text{-CNPyr}]^-$	2-cianopyrrolide
$[(C_1O)PHO_2]^-$	methylphosphonate
$[C_1SO_3]^-$	methylsulfonate
$[C_1SO_4]^-$	methylsulfate
$[C_2SO_4]^-$	ethylsulfate
$[DCA]^-$	dicyanamide
$[(C_2O)_2PO_2]^-$	diethyl phosphate
$[Im]^-$	imidazolate
$[Lys]^-$	lysinate
$[NO_3]^-$	nitrate
$[NTf_2]^-$	bis(trifluoromethylsulfonyl)imide
$[OAc]^-$	acetate
$[OTf]^-$	trifluoromethanesulfonate
$[PF_6]^-$	hexafluorophosphate
$[Pro]^-$	prolinate
$[SCN]^-$	thiocyanate
$[Suc]^-$	succinate
$[Tau]^-$	taurine
$[TCM]^-$	tricyanomethanide
$[Threo]^-$	threonine

Techniques

COSY	$^1H,^1H$-correlation spectroscopy
CP	cross polarization
DFT	density functional theory
DOSY	diffusion ordered spectroscopy
FSLG-HETCOR	frequency-switched Lee-Goldburg—dipolar heteronuclear correlation
HMBC	heteronuclear multiple bond correlation
HSQC	heteronuclear single quantum coherence
HOESY	heteronuclear nuclear Overhauser effect spectroscopy
INADEQUATE	incredible natural abundance double quantum transfer experiment
INEPT	insensitive nuclei enhanced by polarization transfer
IR	infrared
FT	Fourier-transform
MAS	magic angle spinning
MD	molecular dynamic
NMR	nuclear magnetic resonance
NOE	nuclear Overhauser effect
NOESY	nuclear Overhauser effect spectroscopy

PFG	pulsed field gradient
PLM	polarized light microscopy
PTNMR	polarization transfer NMR
ssNMR	solid state nuclear magnetic resonance
XRD	X-ray diffraction

Author details

Mónica M. Lopes[1], Raquel V. Barrulas[1], Tiago G. Paiva[1], Ana S. D. Ferreira[2], Marcileia Zanatta[1] and Marta C. Corvo[1*]

1 School of Science and Technology, Materials Science Department, i3N|Cenimat, NOVA University Lisbon, Caparica, Portugal

2 School of Science and Technology, Chemistry Department, UCIBIO, NOVA University Lisbon, Caparica, Portugal

*Address all correspondence to: marta.corvo@fct.unl.pt

References

[1] Hayes R, Warr GG, Atkin R. Structure and nanostructure in ionic liquids. Chemical Reviews. 2015;**115**:6357-6426. DOI: 10.1021/cr500411q

[2] Damodaran K. Recent NMR studies of ionic liquids. In: Annual Reports on NMR Spectroscopy. Elsevier. 2016. Vol. 88 pp. 215-244. DOI: 10.1016/bs.arnmr.2015.11.002

[3] Nanda R, Damodaran K. A review of NMR methods used in the study of the structure and dynamics of ionic liquids. Magnetic Resonance in Chemistry. 2018;**56**:62-72. DOI: 10.1002/mrc.4666

[4] Zheng YZ, Wang NN, Luo JJ, Zhou Y, Yu ZW. Hydrogen-bonding interactions between [BMIM][BF4] and acetonitrile. Physical Chemistry Chemical Physics. 2013;**15**:18055-18064. DOI: 10.1039/c3cp53356e

[5] Wang H, Cui J, Li H, Zhao Y, Wang J. The effect of cationic structure of ionic liquids on their interactions with 5-hydroxymethylfurfural. Journal of Molecular Structure. 2019;**1179**:57-64. DOI: 10.1016/j.molstruc.2018.10.093

[6] Khatun S, Castner EW. Ionic liquid-solute interactions studied by 2D NOE NMR spectroscopy. The Journal of Physical Chemistry. B. 2015;**119**:9225-9235. DOI: 10.1021/jp509861g

[7] Castiglione F, Appetecchi GB, Passerini S, Panzeri W, Indelicato S, Mele A. Multiple points of view of heteronuclear NOE: Long range vs short range contacts in pyrrolidinium based ionic liquids in the presence of Li salts. Journal of Molecular Liquids. 2015;**210**:215-222. DOI: 10.1016/j.molliq.2015.05.036

[8] Castiglione F, Famulari A, Raos G, Meille SV, Mele A, Appetecchi GB, et al. Pyrrolidinium-based ionic liquids doped with lithium salts: How does Li+ coordination affect its diffusivity? The Journal of Physical Chemistry. B. 2014;**118**:13679-13688. DOI: 10.1021/jp509387r

[9] Sebastião RCO, Pacheco CN, Braga JP, Piló-Veloso D. Diffusion coefficient distribution from NMR-DOSY experiments using Hopfield neural network. Journal of Magnetic Resonance. 2006;**182**:22-28. DOI: 10.1016/j.jmr.2006.06.005

[10] Kaintz A, Baker G, Benesi A, Maroncelli M. Solute diffusion in ionic liquids, NMR measurements and comparisons to conventional solvents. The Journal of Physical Chemistry. B. 2013;**117**:11697-11708. DOI: 10.1021/jp405393d

[11] Garaga MN, Nayeri M, Martinelli A. Effect of the alkyl chain length in 1-alkyl-3-methylimidazolium ionic liquids on inter-molecular interactions and rotational dynamics. Journal of Molecular Liquids. 2015;**210**:169-177. DOI: 10.1016/j.molliq.2015.06.055

[12] Rumble CA, Kaintz A, Yadav SK, Conway B, Araque JC, Baker GA, et al. Rotational dynamics in ionic liquids from NMR relaxation experiments and simulations: Benzene and 1-ethyl-3-methylimidazolium. The Journal of Physical Chemistry. B. 2016;**120**:9450-9467. DOI: 10.1021/acs.jpcb.6b06715

[13] Rumble CA, Uitvlugt C, Conway B, Maroncelli M. Solute rotation in ionic liquids: Size, shape, and electrostatic effects. The Journal of Physical Chemistry. B. 2017;**121**:5094-5109. DOI: 10.1021/acs.jpcb.7b01704

[14] Potdar S, Anantharaj R, Banerjee T. Aromatic extraction using mixed ionic liquids: Experiments and COSMO-RS predictions. Journal of Chemical and

Engineering Data. 2012;**57**:1026-1035. DOI: 10.1021/je200924e

[15] Revelli AL, Mutelet F, Jaubert JN. Extraction of benzene or thiophene from n-heptane using ionic liquids. NMR and thermodynamic study. The Journal of Physical Chemistry. B. 2010;**114**:4600-4608. DOI: 10.1021/jp911978a

[16] Kumar AAP, Banerjee T. Thiophene separation with ionic liquids for desulphurization: A quantum chemical approach. Fluid Phase Equilibria. 2009;**278**:1-8. DOI: 10.1016/j.fluid.2008.11.019

[17] Dias N, Shimizu K, Morgado P, Filipe EJM, Canongia Lopes JN, Vaca Chávez F. Charge templates in aromatic plus ionic liquid systems revisited: NMR experiments and molecular dynamics simulations. The Journal of Physical Chemistry. B. 2014;**118**:5772-5780. DOI: 10.1021/jp503130y

[18] Shimizu K, Gomes MFC, Padua AAH, Rebelo LPN, Lopes JNC. On the role of the dipole and quadrupole moments of aromatic compounds in the solvation by ionic liquids. The Journal of Physical Chemistry. B. 2009;**113**:9894-9900. DOI: 10.1021/jp903556q

[19] Su B-MM, Zhang S, Zhang ZC. Structural elucidation of thiophene interaction with ionic liquids by multinuclear NMR spectroscopy. The Journal of Physical Chemistry. B. 2004;**108**:19510-19517. DOI: 10.1021/jp049027l

[20] Barrulas RV, Paiva TG, Corvo MC. NMR methodology for a rational selection of ionic liquids: Extracting polyphenols. Separation and Purification Technology. 2019;**221**:29-37. DOI: 10.1016/j.seppur.2019.03.077

[21] Román-Leshkov Y, Barrett CJ, Liu ZY, Dumesic JA. Production of dimethylfuran for liquid fuels from biomass-derived carbohydrates. Nature. 2007;**447**:982-985. DOI: 10.1038/nature05923

[22] Wang NN, Zhang QG, Wu FG, Li QZ, Yu ZW. Hydrogen bonding interactions between a representative pyridinium-based ionic liquid [BuPy][BF4] and water/dimethyl sulfoxide. The Journal of Physical Chemistry. B. 2010;**114**:8689-8700. DOI: 10.1021/jp103438q

[23] Perinu C, Arstad B, Jens K-J. NMR spectroscopy applied to amine–CO_2–H_2O systems relevant for post-combustion CO_2 capture: A review. International Journal of Greenhouse Gas Control. 2014;**20**:230-243. DOI: 10.1016/J.IJGGC.2013.10.029

[24] Corvo MC, Sardinha J, Menezes SC, Einloft S, Seferin M, Dupont J, et al. Solvation of carbon dioxide in [c4mim][bf4] and [c4mim][pf6] ionic liquids revealed by high-pressure NMR spectroscopy. Angewandte Chemie, International Edition. 2013;**52**:13024-13027. DOI: 10.1002/anie.201305630

[25] Corvo MC, Sardinha J, Casimiro T, Marin G, Seferin M, Einloft S, et al. A rational approach to CO_2 capture by imidazolium ionic liquids: Tuning CO_2 solubility by cation alkyl branching. ChemSusChem. 2015;**8**:1935-1946. DOI: 10.1002/cssc.201500104

[26] Allen J, Damodaran K. High-resolution slice selection NMR for the measurement of CO_2 diffusion under non-equilibrium conditions. Magnetic Resonance in Chemistry. 2015;**53**:200-202. DOI: 10.1002/mrc.4176

[27] Blath J, Deubler N, Hirth T, Schiestel T. Chemisorption of carbon dioxide in imidazolium based ionic liquids with carboxylic anions. Chemical Engineering Journal. 2012;**181-182**:152-158. DOI: 10.1016/j.cej.2011.11.042

[28] Besnard M, Cabaço MI, Vaca Chávez F, Pinaud N, Sebastião PJ,

Coutinho JAP, et al. CO_2 in 1-butyl-3-methylimidazolium acetate. 2. NMR investigation of chemical reactions. The Journal of Physical Chemistry. A. 2012;**116**:4890-4901. DOI: 10.1021/jp211689z

[29] Cabaço MI, Besnard M, Chávez FV, Pinaud N, Sebastião PJ, Coutinho JAP, et al. Understanding chemical reactions of CO_2 and its isoelectronic molecules with 1-butyl-3-methylimidazolium acetate by changing the nature of the cation: The case of CS_2 in 1-butyl-1-methylpyrrolidinium acetate studied by NMR spectroscopy and density functional theory calculations. The Journal of Chemical Physics. 2014;**140**:244307. DOI: 10.1063/1.4884820

[30] Kortunov PV, Baugh LS, Siskin M. Pathways of the chemical reaction of carbon dioxide with ionic liquids and amines in ionic liquid solution. Energy and Fuels. 2015;**29**:5990-6007. DOI: 10.1021/acs.energyfuels.5b00876

[31] Umecky T, Abe M, Takamuku T, Makino T, Kanakubo M. CO_2 absorption features of 1-ethyl-3-methylimidazolium ionic liquids with 2,4-pentanedionate and its fluorine derivatives. Journal of CO_2 Utilization. 2019;**31**:75-84. DOI: 10.1016/j.jcou.2019.02.020

[32] Seo S, Quiroz-Guzman M, Gohndrone TR, Brennecke JF. Comment on Selective chemical separation of carbon dioxide by ether functionalized imidazolium cation based ionic liquids. In: Sharma P, Choi SH, Park Sd, Baek IH, and Lee GS, editors. The Chemical Engineering Journal. 2012;**181-182**: 834-841. The Chemical Engineering Journal. 2014;**245**:367-369. DOI:10.1016/j.cej.2013.08.051

[33] Sharma P, Choi SH, Do Park S, Baek IH, Lee GS. Selective chemical separation of carbondioxide by ether functionalized imidazolium cation based ionic liquids. Chemical Engineering Journal. 2012;**181-182**: 834-841. DOI: 10.1016/j.cej.2011.12.024

[34] Bates ED, Mayton RD, Ntai I, Davis JH. CO_2 capture by a task-specific ionic liquid. Journal of the American Chemical Society. 2002;**124**:926-927. DOI: 10.1021/ja017593d

[35] Kortunov PV, Siskin M, Baugh LS, Calabro DC. In situ nuclear magnetic resonance mechanistic studies of carbon dioxide reactions with liquid amines in non-aqueous systems: Evidence for the formation of carbamic acids and zwitterionic species. Energy and Fuels. 2015;**29**:5940-5966. DOI: 10.1021/acs.energyfuels.5b00985

[36] Kortunov PV, Siskin M, Baugh LS, Calabro DC. In situ nuclear magnetic resonance mechanistic studies of carbon dioxide reactions with liquid amines in aqueous systems: New insights on carbon capture reaction pathways. Energy and Fuels. 2015;**29**:5919-5939. DOI: 10.1021/acs.energyfuels.5b00850

[37] Bhattacharyya S, Shah FU. Ether functionalized choline tethered amino acid ionic liquids for enhanced CO_2 capture. ACS Sustainable Chemistry and Engineering. 2016;**4**:5441-5449. DOI: 10.1021/acssuschemeng.6b00824

[38] Bhattacharyya S, Filippov A, Shah FU. Insights into the effect of CO_2 absorption on the ionic mobility of ionic liquids. Physical Chemistry Chemical Physics. 2016;**18**:28617-28625. DOI: 10.1039/C6CP05804C

[39] Chen Y, Zhou XQ, Cao Y, Xue Z, Mu T. Quantitative investigation on the physical and chemical interactions between CO_2 and amine-functionalized ionic liquid [aEMMIM][BF 4] by NMR. Chemical Physics Letters. 2013;**574**:124-128. DOI: 10.1016/j.cplett.2013.04.069

[40] Filippov A, Bhattacharyya S, Shah FU. CO_2 absorption and ion mobility in aqueous choline-based ionic liquids. Journal of Molecular Liquids. 2019;**276**:748-752. DOI: 10.1016/J.MOLLIQ.2018.12.045

[41] Goodrich BF, de la Fuente JC, Gurkan BE, Lopez ZK, Price EA, Huang Y, et al. Effect of water and temperature on absorption of CO_2 by amine-functionalized anion-tethered ionic liquids. The Journal of Physical Chemistry. B. 2011;**115**:9140-9150. DOI: 10.1021/jp2015534

[42] Seo S, Quiroz-Guzman M, Desilva MA, Lee TB, Huang Y, Goodrich BF, et al. Chemically tunable ionic liquids with aprotic heterocyclic anion (AHA) for CO_2 capture. The Journal of Physical Chemistry. B. 2014;**118**:5740-5751. DOI: 10.1021/jp502279w

[43] Huang Y, Cui G, Zhao Y, Wang H, Li Z, Dai S, et al. Preorganization and cooperation for highly efficient and reversible capture of low-concentration CO_2 by ionic liquids. Angewandte Chemie, International Edition. 2017;**56**:13293-13297. DOI: 10.1002/anie.201706280

[44] Huang Y, Cui G, Wang H, Li Z, Wang J. Tuning ionic liquids with imide-based anions for highly efficient CO_2 capture through enhanced cooperations. Journal of CO_2 Utilization. 2018;**28**:299-305. DOI: 10.1016/J.JCOU.2018.10.013

[45] Zanatta M, Simon NM, dos Santos FP, Corvo MC, Cabrita EJ, Dupont J. Correspondence on "preorganization and cooperation for highly efficient and reversible capture of low-concentration CO_2 by ionic liquids". Angewandte Chemie, International Edition. 2019;**58**:382-385. DOI: 10.1002/anie.201712252

[46] McDonald JL, Sykora RE, Hixon P, Mirjafari A, Davis JH. Impact of water on CO_2 capture by amino acid ionic liquids. Environmental Chemistry Letters. 2014;**12**:201-208. DOI: 10.1007/s10311-013-0435-1

[47] Filippov A, Antzutkin ON, Shah FU. Reactivity of CO_2 with aqueous choline-based ionic liquids probed by solid-state NMR spectroscopy. Journal of Molecular Liquids. 2019;**286**:110918. DOI: 10.1016/J.MOLLIQ.2019.110918

[48] Simon NM, Zanatta M, dos Santos FP, Corvo MC, Cabrita EJ, Dupont J. Carbon dioxide capture by aqueous ionic liquid solutions. ChemSusChem. 2017;**10**:4927-4933. DOI: 10.1002/cssc.201701044

[49] Simon NM, Zanatta M, Neumann J, Girard A-L, Marin G, Stassen H, et al. Cation–anion–CO_2 interactions in imidazolium-based ionic liquid sorbents. ChemPhysChem. 2018;**19**:2879-2884. DOI: 10.1002/cphc.201800751

[50] Kafy A, Ko H-U, Kim HC, Mun S, Zhai L, Kim J. Renewable smart materials. Smart Materials and Structures. 2016;**25**:073001. DOI: 10.1088/0964-1726/25/7/073001

[51] Alves L, Medronho B, Filipe A, E. Antunes F, Lindman B, Topgaard D, et al. New insights on the role of urea on the dissolution and thermally-induced gelation of cellulose in aqueous alkali. Gels. 2018;**4**:87. DOI: 10.3390/gels4040087

[52] Huang H, Ge H, Song J, Yao Y, Chen Q, Xu M. NMR study on the roles of Li+ in the cellulose dissolution process. ACS Sustainable Chemistry and Engineering. 2019;**7**:618-624. DOI: 10.1021/acssuschemeng.8b04177

[53] Ru G, Wu S, Yan X, Liu B, Gong P, Wang L, et al. Inverse solubility of chitin/

chitosan in aqueous alkali solvents at low temperature. Carbohydrate Polymers. 2019;**206**:487-492. DOI: 10.1016/j.carbpol.2018.11.016

[54] Xu K, Xiao Y, Cao Y, Peng S, Fan M, Wang K. Dissolution of cellulose in 1-allyl-3-methylimidazolium methyl phosphonate ionic liquid and its composite system with Na_2PHO_3. Carbohydrate Polymers. 2019;**209**:382-388. DOI: 10.1016/j.carbpol.2018.12.040

[55] Minnick DL, Flores RA, DeStefano MR, Scurto AM. Cellulose solubility in ionic liquid mixtures: Temperature, cosolvent, and antisolvent effects. The Journal of Physical Chemistry. B. 2016;**120**:7906-7919. DOI: 10.1021/acs.jpcb.6b04309

[56] Zhang C, Kang H, Li P, Liu Z, Zhang Y, Liu R, et al. Dual effects of dimethylsulfoxide on cellulose solvating ability of 1-allyl-3-methylimidazolium chloride. Cellulose. 2016;**23**:1165-1175. DOI: 10.1007/s10570-016-0876-3

[57] Gentile L, Olsson U. Cellulose–solvent interactions from self-diffusion NMR. Cellulose. 2016;**23**:2753-2758. DOI: 10.1007/s10570-016-0984-0

[58] Paiva T, Echeverria C, Godinho MH, Almeida PL, Corvo MC. On the influence of imidazolium ionic liquids on cellulose derived polymers. European Polymer Journal. 2019;**114**:353-360. DOI: 10.1016/j.eurpolymj.2019.02.032

[59] Kostag M, El Seoud OA. Dependence of cellulose dissolution in quaternary ammonium-based ionic liquids/DMSO on the molecular structure of the electrolyte. Carbohydrate Polymers. 2019;**205**:524-532. DOI: 10.1016/j.carbpol.2018.10.055

[60] Tian D, Li T, Zhang R, Wu Q, Chen T, Sun P, et al. Conformations and intermolecular interactions in cellulose/silk fibroin blend films: A solid-state NMR perspective. The Journal of Physical Chemistry. B. 2017;**121**:6108-6116. DOI: 10.1021/acs.jpcb.7b02838

[61] Saalwächter K, Spiess HW. Solid-state NMR of polymers. In: Polymer Science: A Comprehensive Reference. Vol. 10. Amsterdam: Elsevier; 2012. pp. 185-219. DOI: 10.1016/B978-0-444-53349-4.00025-X

[62] Niedermeyer H, Hallett JP, Villar-Garcia IJ, Hunt PA, Welton T. Mixtures of ionic liquids. Chemical Society Reviews. 2012;**41**:7780. DOI: 10.1039/c2cs35177c

[63] Chatel G, Pereira JFB, Debbeti V, Wang H, Rogers RD. Mixing ionic liquids—"Simple mixtures" or "double salts"? Green Chemistry. 2014;**16**:2051. DOI: 10.1039/c3gc41389f

[64] Lui MY, Crowhurst L, Hallett JP, Hunt PA, Niedermeyer H, Welton T. Salts dissolved in salts: Ionic liquid mixtures. Chemical Science. 2011;**2**:1491. DOI: 10.1039/c1sc00227a

[65] Iglesias-Otero MA, Troncoso J, Carballo E, Romaní L. Density and refractive index in mixtures of ionic liquids and organic solvents: Correlations and predictions. The Journal of Chemical Thermodynamics. 2008;**40**:949-956. DOI: 10.1016/j.jct.2008.01.023

[66] Reddy PN, Padmaja P, Subba Reddy BV, Rambabu G. Ionic liquid/water mixture promoted organic transformations. RSC Advances. 2015;**5**:51035-51054. DOI: 10.1039/C5RA08625F

[67] Rodríguez H, Rogers RD. Liquid mixtures of ionic liquids and polymers as solvent systems. Fluid Phase Equilibria. 2010;**294**:7-14. DOI: 10.1016/j.fluid.2009.12.036

[68] MacFarlane DR, Chong AL, Forsyth M, Kar M, Vijayaraghavan R, Somers A, et al. New dimensions in salt–solvent mixtures: A 4th evolution of ionic liquids. Faraday Discussions. 2018;**206**:9-28. DOI: 10.1039/C7FD00189D

[69] Canongia Lopes JN, Cordeiro TC, Esperança JMSS, Guedes HJR, Huq S, Rebelo LPN, et al. Deviations from ideality in mixtures of two ionic liquids containing a common ion. The Journal of Physical Chemistry. B. 2005;**109**: 3519-3525. DOI: 10.1021/jp0458699

[70] Omar S, Lemus J, Ruiz E, Ferro VR, Ortega J, Palomar J. Ionic liquid mixtures—An analysis of their mutual miscibility. The Journal of Physical Chemistry. B. 2014;**118**: 2442-2450. DOI: 10.1021/jp411527b

[71] Fillion JJ, Brennecke JF. Viscosity of ionic liquid–ionic liquid mixtures. Journal of Chemical and Engineering Data. 2017;**62**:1884-1901. DOI: 10.1021/acs.jced.7b00221

[72] Matthews RP, Villar-Garcia IJ, Weber CC, Griffith J, Cameron F, Hallett JP, et al. structural investigation of ionic liquid mixtures. Physical Chemistry Chemical Physics. 2016;**18**:8608-8624. DOI: 10.1039/C6CP00156D

[73] Marullo S, D'Anna F, Campodonico PR, Noto R. Ionic liquid binary mixtures: How different factors contribute to determine their effect on the reactivity. RSC Advances. 2016;**6**: 90165-90171. DOI: 10.1039/C6RA12836J

[74] Zhou Y, Qu J. Ionic liquids as lubricant additives: A review. ACS Applied Materials and Interfaces. 2017;**9**:3209-3222. DOI: 10.1021/acsami.6b12489

[75] Filippov A, Azancheev N, Gibaydullin A, Bhattacharyya S, Antzutkin ON, Shah FU. Dynamic properties of imidazolium orthoborate ionic liquids mixed with polyethylene glycol studied by NMR diffusometry and impedance spectroscopy. Magnetic Resonance in Chemistry. 2018;**56**: 113-119. DOI: 10.1002/mrc.4636